ChemComm

View Online
Dynamic Article Links

Cite this: *Chem. Commun.*, 2011, **47**, 5476–5478

www.rsc.org/chemcomm

COMMUNICATION

Electrochemical sensing of L-histidine based on structure-switching DNAzymes and gold nanoparticle–graphene nanosheet composites†

Junfei Liang,‡ Zhengbo Chen,‡ Lin Guo* and Lidong Li*

Received 18th February 2011, Accepted 25th March 2011
DOI: 10.1039/c1cc10965k

A sensitive aptasensor for detection of L-histidine based on the switching structure of aptamer and gold nanoparticles–graphene nanosheets (GNPs–GNSs) composite was reported for the first time. The fabricated biosensor shows an expanded linear range, excellent sensitivity and selectivity against other amino acids.

L-Histidine is one of the naturally occurring amino acids. It plays a very active role in many biological systems.[1–3] It acts as a neurotransmitter or neuromodulator in the mammalian central nervous system, including the retina.[4,5] It can minimize internal bleeding from microtrauma.[6] A persistent L-histidine deficiency causes Friedreich ataxia, epilepsy, Parkinson's disease, and the failure of normal erythropoiesis development.[7,8] Thus, the determination of L-histidine in biological fluids is of great importance for biological studies.

Several sophisticated technologies including sensors/biosensors,[9,10] potentiometry,[11] fluorescence with capillary electrophoresis,[12] voltammetry,[9] mass-spectrometry,[13] chromatography[14] and spectroscopy,[15] have been used for L-histidine detection. However, use of large sample volumes, expensive instrumentation, lack of reproducibility and selectivity, and eco-unfriendly solvents are serious concerns associated with these techniques. Aptamer-based sensors have emerged as a promising and versatile biosensor platform.[16,17]

Graphene, a one-atom thick and two-dimensional closely packed honeycomb lattice, has received numerous investigations from both the experimental and theoretical scientific communities, since the experimental observation of single layers by Novoselov and Geim in 2004.[18] Very recently, Rusling *et al.* reported an electrochemical immunosensor by using enzyme label horseradish peroxidase (HRP)-CNTs. In their protocol, before bioconjugation, the oxidized MWNTs on mica was of thickness 25 ± 2 nm.[19] In comparison with carbon nanotubes (CNTs) as a support for electrochemical biosensors, graphene possesses very small thickness, good thermal conductivity, electrical conductivity, mechanical strength and larger surface area than CNTs. Therefore graphene is a very promising candidate for new carbonaceous supports.

Meanwhile, the integration of graphene with noble metal nanoparticles is relatively new in biosensor applications. Despite the sparse demonstration of GNPs–GNSs composites for biosensing applications,[20,21] proposed biosensors based on switching structure of aptamer and GNPs–GNSs have not been reported.

Here we report a sensitive aptasensor for detection of L-histidine based on switching structure of aptamer and GNPs–GNSs composite for the first time. First GNPs–GNSs were synthesized, by depositing GNPs on the surface of the GNPs through spontaneous chemical reduction of chloroauric acid by sodium citrate, and a glassy carbon electrode (GCE) was modified with GNPs–GNSs. Then, thiolated DNA duplex was immobilized onto the GNPs *via* sulfur–gold affinity (see ESI†). The introduction of L-histidine induced self-cleavage of DNAzyme on the GNPs–GNSs/GCE and the ferrocene (Fc) redox marker approached the electrode surface and produced measurable electrochemical signals. Because of the excellent conductivity and high specific surface area of graphene, the good distribution of GNPs on GNSs leads to the fabricated L-histidine biosensor showing an expanded linear range and excellent sensitivity. An expanded linear electrical response was observed for concentrations ranging from 10 pM to 10 μM, and a low detection limit of 0.1 pM L-histidine was achieved, and fast response speed was obtained. Meanwhile, the proposed approach exhibited excellent selectivity against other amino acids. Such an aptasensor provides a promising strategy for screening other amino acids and toxic ions at ultratrace levels on-line. The results demonstrate that the GNPs–GNSs composite can offer a new and promising material for aptasensor designs.

The proposed aptasensor consists of an Fc modified version of the catalytic DNA(2) strand, which is composed of a functional domain of 24 deoxynucleotides flanked by 5′ and 3′ substrate-recognition domains of 8 nucleotides each, hybridized to its sequence-specific nuclease acting on a single-stranded DNA substrate containing a single, sessile riboadenine (indicated by arrows in Scheme 1). In the absence of L-histidine, this duplex architecture, which is chemi-anchored to GNPs–GNSs *via* a 3′ terminal thiol on the catalytic strand, is relatively rigid, presumably preventing the Fc from approaching the GCE to transfer electrons (Scheme 1, left). In the presence of L-histidine, the *trans*-acting catalytic strand

School of Chemistry & Environment, Beijing University of Aeronautics & Astronautics, Beijing, 100191, P. R. China.
E-mail: guolin@buaa.edu.cn, lilidong@buaa.edu.cn;
Fax: +86-010-82338162; Tel: +86-010-82338162
† Electronic supplementary information (ESI) available: Experimental details. See DOI: 10.1039/c1cc10965k
‡ These authors contributed equally to this work.

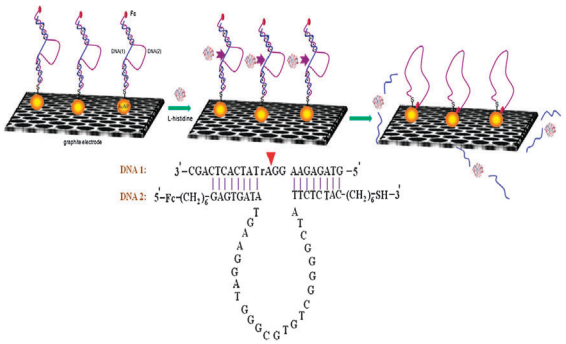

Scheme 1 A schematic representation of the experiment protocol. Inset: secondary structure of L-histidine-dependent DNAzyme employed.

cleaves the sessile phosphodiester of the substrate into two fragments (Scheme 1 middle). The fragments dissociate from the complex, release its partially complementary DNA(2), because the 8-mer DNA strands bind relatively more weakly than the 16 mer duplex strand (generally, the melting point of 8-mer DNA duplex is around room temperature). Therefore, after the dissociation, the ferrocene moiety becomes free to move. Then the DNA(2) place their redox tags in close proximity to the electrode upon folding into their favorable secondary configurations, allowing the Fc to transfer electrons to the electrode and produce measurable electrochemical signals (Scheme 1 right).

A representative XRD pattern of the GNPs–GNSs nanocomposite is shown in Fig. 1. The four peaks with *d* values of 2.36, 2.04, 1.44, 1.23, correspond to (111), (200), (220) and (311) planes, respectively, which are in good agreement with literature values of pure metallic Au (JCPDS, 04-0784).

The structure and substructures of the GNPs–GNSs nanocomposite was further characterized by TEM and high-resolution TEM. From Fig. 2a, it can be seen that all the GNPs are uniformly distributed on the GNSs. GNPs are surrounded by flexible graphene nanosheets, which can be distinguished as linear strips. The size of the GNPs is found to be $\approx$30 nm. The GCE was modified with GNPs–GNSs, and the thiolated DNA duplex was immobilized onto the GNPs *via* the 3′ terminal thiol-gold affinity. The good distribution of GNPs on GNSs make more duplex architectures adsorb on the GNPs and the fabricated biosensor shows an efficiently expanded linear range. Fig. 2b presents a lattice resolved HRTEM image of the GNPs–GNSs nanocomposite, from which the lattice fringes of GNPs are clearly visible. The lattice fringe spacing

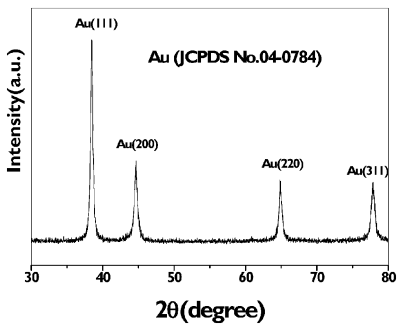

Fig. 1 X-Ray diffraction pattern of GNPs–GNSs nanocomposite.

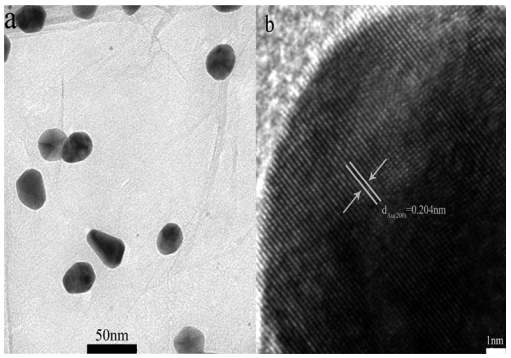

Fig. 2 (a) TEM and (b) HRTEM image of the GNPs–GNSs nanocomposite.

between two adjacent crystal planes of the particle was determined to be 0.204 nm in the HRTEM image, corresponding to the (200) lattice plane of Au.

Raman spectroscopy is a powerful tool to characterize carbonaceous materials. The significant structural changes occurring during the chemical processing from GO to GNSs, and then to the GNPs–GNSs are reflected in their Raman spectra (Fig. 3). The Raman spectrum of GO contains both a G band (1594.6 cm^{-1}, E_{2g} phonon of C sp^2 atoms) and D band (1363.9 cm^{-1}, κ-point phonons of A_{1g} symmetry).[22] The Raman spectra of GNSs and GNPs–GNSs nanocomposites also contain both G and D bands, however, with an increased D/G intensity ratio compared to that in GO. This change suggests a decrease in the average size of the sp^2 domains upon reduction of the exfoliated GO, and can be explained if new graphitic domains were created that are smaller in size to those present in GO before reduction, but more numerous in number. Ruoff *et al.* reported that the conductivity of GNSs reduced by hydrazine was about five orders of magnitude better than the conductivity of GO, and very close to that of pristine graphite.[23] The GNPs–GNSs nanocomposite is suitable for electrochemical analysis because of the excellent conductivity of GNSs.

The self-cleaving DNAzyme-based sensor is sensitive and specific to its target molecule. In order to test signal enhancement for DNAzymes with GNPs–GNSs, square wave voltammetry (SWV) was carried out at the GCE modified by GNPs–GNSs. Fig. 4a depicts SWV profiles for the electrode with DNA duplex modification after reacting with concentrations of

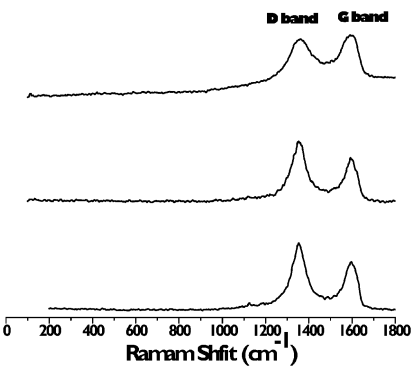

Fig. 3 Raman spectra of GO (top), GNSs (middle) and GNPs–GNSs (bottom).

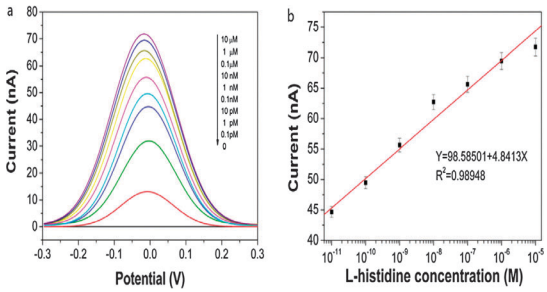

Fig. 4 (a) Typical SWVs of sensing system to different L-histidine concentrations from 0.1 pM to 10 μM. (b) Linear relationship between the peak currents and L-histidine concentration.

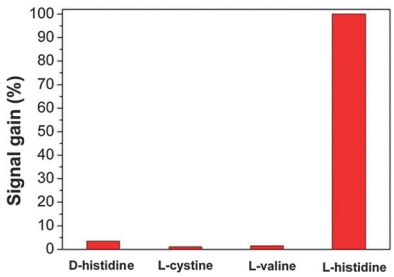

Fig. 5 Relative response of the sensing system to different amino acids.

L-histidine from 0.1 pM to 10 μM. From Fig. 4a, it can be seen that the peak current increases with increasing concentrations of L-histidine as a consequence of the efficient capture of the L-histidine by the aptasensor, and the detection limit of this method is 0.1 pM. The SWV current varies linearly with L-histidine concentration in the range from 10 pM to 10 μM, as depicted in the inset of Fig. 4b. In comparison with a gold electrode for L-histidine the fabricated GNPs–GNSs/GCE electrode shows an wider linear detection range and lower detection limit (see ESI†).

Particularly, the aptasensor reaches equilibration very rapidly, complete saturation of the SWV signal occurs in less than 30 s; presumably the fast response is ascribed to the excellent transport properties of GNSs, the high catalytic activity of the self-cleaving strand DNA(1) with $k_{obs} = 0.2\ min^{-1}$,[24] and the fast equilibrium between the duplex configuration and the favourable secondary structure of DNA(2).

Not only does a biosensor have to be sensitive to different concentrations of the analyte, it must also be specific. The selectivity of the aptasensor was determined by testing it with L-cystine, L-valine and D-histidine, each at 1 μM concentration. As shown in Fig. 5, compared with 0 M L-histidine, for 1 μM L-cystine, L-valine and D-histidine, no significant signal change was observed. This indicates that nonspecific adsorption of the foreign amino acids (L-cystine, L-valine and D-histidine) to the base aptamer does not occur obviously, and the effects of these foreign amino acids on L-histidine detection are almost negligible. The designed aptasensor thus has a clear specificity for L-histidine.

In summary, the proposed sensing protocol exhibits excellent sensitivity and reasonable selectivity for its target molecules. It especially offers amazingly fast speed and operational convenience. The fast response provides a platform for L-histidine detection on-line. Meanwhile, it is a reagentless sensor since both the recognition element (self-cleaving DNAzymes) and the signaling element (Fc) have been integrated in a surface-confined configuration. Especially, it offers a very simple *enantio*-analytical method for L-histidine detection. The results also demonstrate that GNPs–GNSs, with good distribution of GNPs, can provide a promising platform for more aptamer immobilization for target molecule capture than the biosensor without GNPs–GNSs modification. The protocol exhibits an expanded linear range and extreme low detection limit of 0.1 pM with little sample consumption.

This project was financially supported by National Natural Science Foundation of China (50725208 & 20973019) as well as by Specialized Research Fund for the Doctoral Program of Higher Education (20091102110035).

Notes and references

1 R. H. Hol, P. Kennepohl and E. I. Solomon, *Chem. Rev.*, 1996, **96**, 2239.
2 S. Karlin, Z. Y. Zhu and K. D. Karlin, *Proc. Natl. Acad. Sci. U. S. A.*, 1997, **94**, 14225.
3 J. A. Roe, A. Butler, D. M. Scholler, J. S. Valentine, L. Marky and K. J. Breslauer, *Biochemistry*, 1988, **27**, 950.
4 G. N. Chen, X. P. Wu, J. P. Duan and H. Q. Chen, *Talanta*, 1999, **49**, 319.
5 Y. Kusakari, S. Nishikawa, S. Ishiguro and M. Tamai, *Curr. Eye Res.*, 1997, **16**, 600.
6 D. F. Horrobin, M. S. Mandu, M. Oka, R. O. Morgan, S. C. Cunnane, A. I. Aly, T. Ghayur, M. Schweitzer and R. A. Karmali, *Med. Hypotheses*, 1979, **5**, 969.
7 N. M. VanGelder, M. Roy, F. Belanger, S. Paris and A. Barbeau, *Curr. Top. Nutr. Dis.*, 1987, **16**, 271.
8 M. L. Rao, H. Stefan, C. Scheid, A. D. Kuttler and W. Froscher, *Epilepsia*, 1993, **34**, 347.
9 L. C. Chen, C. C. Chang and H. C. Chang, *Electrochim. Acta*, 2008, **53**, 2883.
10 M. Shojaei, A. Mirmohseni and M. Farbodi, *Anal. Bioanal. Chem.*, 2008, **391**, 2875.
11 R. I. S. V. Staden and L. Holo, *Sens. Actuators, B*, 2007, **120**, 399.
12 L. Y. Zhang and M. X. Sun, *J. Chromatogr., A*, 2004, **1040**, 133.
13 M. Miyagi and T. Nakazawa, *Anal. Chem.*, 2008, **80**, 6481.
14 J. Ruta, C. Grosset, C. Ravelet, J. Fize, A. Villet, A. Ravel and E. Peyrin, *J. Chromatogr., B: Anal. Technol. Biomed. Life Sci.*, 2007, **845**, 186.
15 J. K. Lim, Y. Kim, S. Y. Lee and S. W. Joo, *Spectrochim. Acta, Part A*, 2008, **69**, 286.
16 Y. L. Zhang, Y. Wang, H. B. Wang, J. H. Jiang, G. L. Shen, R. Q. Yu and J. H. Li, *Anal. Chem.*, 2009, **81**, 1982.
17 Y. Jin, X. Yao, Q. Liu and J. H. Li, *Biosens. Bioelectron.*, 2007, **22**, 1126.
18 K. S. Novoselov, A. K. Geim, S. V. Morozov, D. Jiang, Y. Zhang, S. V. Dubonos, I. V. Grigorieva and A. A. Firsov, *Science*, 2004, **306**, 666.
19 R. Malhotra, V. Patel, J. P. Vaqué, J. S. Gutkind and J. F. Rusling, *Anal. Chem.*, 2010, **82**, 3118–3123.
20 T. T. Baby, S. S. J. Aravind, T. Arockiadoss, R. B. Rakhi and S. Ramaprabhu, *Sens. Actuators, B*, 2010, **145**, 71.
21 W. J. Hong, H. Bai, Y. X. Xu, Z. Y. Yao, Z. Z. Gu and G. Q. Shi, *J. Phys. Chem. C*, 2010, **114**, 1822.
22 A. C. Ferrari and J. Robertson, *Phys. Rev. B: Condens. Matter*, 2000, **61**, 14095.
23 S. Stankovich, D. A. Dikin, R. D. Piner, K. A. Kohlhaas, A. Kleinhammes, Y. Y. Jia, Y. Wu, S. T. Nguyen and R. S. Ruo, *Carbon*, 2007, **45**, 1558.
24 A. Roth and R. R. Breaker, *Proc. Natl. Acad. Sci. U. S. A.*, 1998, **95**, 6027.

